Mass spectrometry imaging of endogenous metabolites in response to doxorubicin in a novel 3D osteosarcoma cell culture model

PALUBECKAITĖ, Ieva, CROOKS, Lucy <http://orcid.org/0000-0002-3344-8587>, SMITH, David <http://orcid.org/0000-0001-5177-8574>, COLE, Laura <http://orcid.org/0000-0002-2538-6291>, BRAM, Heijs, LE MAITRE, Christine <http://orcid.org/0000-0003-4489-7107>, CLENCH, Malcolm <http://orcid.org/0000-0002-0798-831X> and CROSS, Neil A <http://orcid.org/0000-0003-2055-5815>

Published version

PALUBECKAITĖ, Ieva, CROOKS, Lucy, SMITH, David, COLE, Laura, BRAM, Heijs, LE MAITRE, Christine, CLENCH, Malcolm and CROSS, Neil A (2019). Mass spectrometry imaging of endogenous metabolites in response to doxorubicin in a novel 3D osteosarcoma cell culture model. Journal of Mass Spectrometry.

Mass spectrometry imaging of endogenous metabolites in response to doxorubicin in a novel 3D osteosarcoma cell culture model

Ieva Palubeckaitė [1], Lucy Crooks [2,] David P. Smith[2], Laura M. Cole[2], Heijs Bram[3], Christine Le Maitre[2], Malcolm R. Clench[2] and Neil A. Cross[2*]

[1]Department of Pathology, Leiden University Medical Center, PO BOX 9600, 2300 RC Leiden, the Netherlands.

[2]Centre for Mass Spectrometry Imaging, Biomolecular Sciences Research Centre, Sheffield Hallam University, Howard Street, Sheffield S1 1WB

[3]Center for Proteomics and Metabolomics, Leiden University Medical Center, PO BOX 9600, 2300 RC Leiden, the Netherlands.

[*]Corresponding Author: Dr Neil Cross, Centre for Mass Spectrometry Imaging, Biomolecular Sciences Research Centre, Sheffield Hallam University, Howard Street, Sheffield S1 1WB email: n.cross@shu.ac.uk

Keywords

Osteosarcoma, 3D cell culture, mass spectrometry imaging, doxorubicin, multivariate analysis.

Abstract

Three-dimensional (3D) cell culture is a rapidly emerging field which mimics some of the physiological conditions of human tissues. In cancer biology, it is considered a useful tool in predicting *in vivo* chemotherapy responses compared with conventional two-dimensional cell culture. We have developed a novel 3D cell culture model of osteosarcoma comprised of aggregated proliferative tumour spheroids, which shows regions of tumour heterogeneity formed by aggregated spheroids of polyclonal tumour cells. Aggregated spheroids show local necrotic and apoptotic regions, and have sizes suitable for the study of spatial distribution of metabolites by mass spectrometry imaging (MSI). We have used this model to perform a proof-of-principle study showing a heterogeneous distribution of endogenous metabolites that co-localise with the necrotic core and apoptotic regions in this model. Cytotoxic chemotherapy (Doxorubicin) responses were significantly attenuated in our 3D cell culture model compared with standard cell culture, as determined by Resazurin assay, despite sufficient doxorubicin diffusion demonstrated by localisation throughout the 3D constructs. Finally, changes to the distribution of endogenous metabolites in response to Doxorubicin were readily detected by MSI. Principle component analysis identified 50 metabolites which differed most in their abundance between treatment groups, and of these, 10 were identified by both in-software *t test* and mixed effects ANOVA. Subsequent independent MSI of identified species were consistent with principle component analysis findings. This proof-of-principle study shows for the first time that chemotherapy-induced changes in metabolite abundance and distribution may be determined in 3D cell culture by MSI, highlighting this method as a potentially useful tool in elucidation of chemotherapy responses as an alternative to *in vivo* testing.

1 Introduction

The current process of drug discovery and development, based on standard cell culture *in vitro* assays followed immediately by *in vivo* studies has produced many effective drug candidates, however this workflow has limitations. Cells grown in standard or 2-dimensional cultures (2D) do not reflect the environment within tumours, which contain heterogeneous cellular environments, with proliferative, quiescent, apoptotic and necrotic regions resulting from oxygen and nutrient-deprivation. Within tumours, oxygen and nutrient deprivation is in-part due to chaotic vasculature and/or considerable extracellular matrix deposition, leading to impaired drug delivery to tumours. In contrast cells in 2D culture receive optimal oxygen, growth factors, and in the case of therapeutics studies, equal drug concentrations equating to that in the medium. The study of drug distributions and effects on downstream pathways via metabolomics approaches have successfully been used to predict anti-tumour cytotoxic responses by the analysis of extracellular metabolites in cancer patients.[1-2] These metabolomic studies have been extended to 3-dimensional (3D) cell culture studies, whereby the environment recapitulates the drug resistance seen *in vivo*,[3-4] and have further shown that metabolomic profiles may predict the malignant potential of cells grown in 3D cell culture.[5]

Numerous 3D cell culture models for the study of drug responses have been developed, however many of these are unsuited to spatial localisation studies due to the small size of resulting cell constructs. Sodium alginate, a naturally occurring polysaccharide extracted from algae, which following chelation with Ca^{2+}, forms cross-links creating a scaffold, and has been used previously for 3D culture of cancerous cells.[6] This method has the advantage of being a clonal grown model dependent on the colony-forming ability of cancer cells, which is a key characteristic of cancer stem cells or tumour initiating cells.[7] However, in this model, spheres develop slowly, and few spheres reach over 400µm diameter, which is insufficient for spatial investigation of molecular distribution by most MSI modalities.[8]

Multicellular tumour spheroids (MCTS) are formed through use of ultra-low adherence techniques, which allows the generation of larger, uniform spheres through aggregation, rather than proliferation, with the possibility of constructs around 1mm size.[8] MCTS models show clear hypoxic cores, apoptotic, quiescent and viable regions representative of tumours,

and both metabolites and proteins have been successfully imaged within 3D cell cultures by MALDI-MSI.[9] Furthermore, MALDI-MSI of metabolite distribution is possible, with species localised to viable and hypoxic core regions in MCTS generated in low-adherence wells.[10] MALDI-MSI-based metabolite distribution in pellet cultures of chondrocytes show varying spatial distributions in hypoxic *vs.* normoxic regions, further supported by pellet cultures generated in hypoxic conditions.[11] MALDI-MSI has also successfully demonstrated spatial and temporal drug distribution (irinotecan, leucovorin, and its metabolites) in 3D MCTS cultures,[12] and irinotecan distributions in patient-derived organoids.[13] Although patient-derived 'organoid' models better represent patient tumours than cell line models and are in development for sarcoma,[14] these are only well developed for epithelial cancers. Suitable osteosarcoma cell line-based 3D models to allow disease-relevant *in vitro* drug responses, including MSI studies, are required.

Since many 3D cell culture models such as MCTS are aggregation models, rather than clonal proliferation models, these may not fully recapitulate the heterogeneous nature of tumours. Even within apparently homogeneous established cell lines, heterogeneous populations exist, and adjacent clones of cells may respond differently to the same cytotoxic stimuli.[15] To circumvent these limitations, we have developed an aggregated spheroid model, creating large constructs of ~1mm diameter from isolated, clonal tumour spheres generated from an alginate bead culture. This creates a tissue construct that is a) sufficiently large for spatial distribution studies by MSI, b) contains a necrotic core, apoptotic and viable regions and c) contains intra-tumoural heterogeneity.

Doxorubicin was chosen to observe drug distribution and identify the metabolomic and lipidomic response of the 3D cell culture. Doxorubicin is an anthracycline which interferes with DNA transcription and replication through the stabilisation of topoisomerase II. Doxorubicin is one of the most widely used drugs for the treatment of high-grade osteosarcoma.[16] In this study, we performed a proof-of-principle study to test whether a heterogeneous metabolite distribution could be detected by MSI, and to image Doxorubicin-induced changes in metabolite changes in response to cytotoxic chemotherapy in 3D cell culture.

2 Methods and Materials

Cell culture

The SAOS-2 osteosarcoma cell line was obtained from American Type Culture Collection (ATCC) and cultured in MEMα (Lonza Ltd, Switzerland) containing 10% foetal bovine serum (FBS) and 10 U/ml penicillin and 10 μg/mL streptomycin (Thermo Scientific, USA). It was maintained in a humidified atmosphere containing 5% CO_2 at 37^{o}C.

3D cell culture

Following expansion in a monolayer, cell lines were suspended in 1.2% w/v medium viscosity alginic acid (Sigma-Aldrich, UK) in 0.15M NaCl at 1x 10^5 cells/mL. Alginate beads were formed via dropping the cellular suspension in 1.2% w/v alginate/0.15 M NaCl (Sigma-Aldrich, UK) through a 19-gauge needle into 0.2 M $CaCl_2$ (Sigma-Aldrich, UK). After incubation at 37^{o}C for 12 minutes, alginate beads were washed twice with 0.15 M NaCl and washed twice in complete media before being placed in the appropriate culture media for 28 days. To release clonal tumour spheres from the alginate matrix, alginate beads were dissolved in 500 μL dissolving buffer per bead (55 mM sodium citrate (Sigma-Aldrich, UK), 30mM EDTA (Sigma-Aldrich, UK), 0.15 M NaCl) for 10 minutes at 37^{o}C with agitation. Following centrifugation, spheroids were immediately placed in 1% agarose-coated (non-adherent) 96 well plates and cultured for a further 7 days.

Chemotherapeutic treatment of 2D and 3D cultures

Once confluent, SAOS-2 osteosarcoma cells were trypsinised and seeded into 96-well plates at 5x10^4 cells/mL. These were allowed to adhere for 24 hours before treatment. Cells were treated with 0-12.8 μM Doxorubicin hydrochloride (Sigma-Aldrich, UK), or 0-4 μM for 3D cell culture studies, for up to 48 hours, with treatment media replaced every 24 hours, for 3 independent cell culture experiments. To assess cell activity/survival during treatment a Resazurin assay was used. Resazurin (Sigma-Aldrich, UK) stock was made at 3mg/mL in αMEM media. Resazurin diluted in complete media (200 μL of 0.3 mg/mL) was added to each well and incubated for 1.5 hours (2D culture) or 3 hours (3D culture) at 37^{o}C, wrapped in foil to protect from light exposure. The fluorescence was recorded using a 530 nm excitation/590 nm emission filter set using a Clariostar microplate reader (BMG Labtech Ltd, UK). After reading the plates the cultures were washed twice with culture medium and cultured further until the last remaining time point. Additionally, doxorubicin controls were

tested in order to confirm the absence of fluorescent interference with the assay. The Resazurin fluorescence values were shown to deviate from the normal distribution by the Shapiro-Wilk test of normality. Therefore, the Kruskal-Wallis test was used to determine if there was a significant difference between Doxorubicin treatments. The Dwass-Steel-Chritchlow-Fligner *post-hoc* test was performed for all pairwise comparisons when a significant difference was observed between treatment groups. When a decrease in cell survival at higher doses was observed, a non-linear regression of (variable) on $\log_{10}$ dose was fit with four parameters in GraphPad Prism (v7) (GraphPad Software, USA).

Fluorescent imaging of spheroid aggregates

To visualise drug distribution in spheroid aggregates, cells were treated with 1 µM Doxorubicin for 6 hours then stained for 25 mins with Hoechst 33342 (10 µg/mL). The fluorescence was visualised on an Olympus IX81 microscope with an Olympus XM10 camera using Texas Red and DAPI channels respectively and analysed using Olympus Cell^F software (Olympus, Germany). Apoptosis was visualised using NucView 488 Caspase-3 fluorogenic substrate (Biotium, Cambridge Research, UK) as per manufacturers' instructions, then counterstained with Hoechst 33342 as above. Necrotic regions were identified by staining simultaneously with Propidium Iodide and Hoechst 33342 staining (both 10 µg/mL).

MALDI-MSI and detection of Doxorubicin in 3D cell culture

A doxorubicin standard-spiked cell plug array was made to aid detection of doxorubicin inside a spheroid using MALDI-MSI to mimic the signal suppression effects in the samples. A gelatin block was made by pouring 20% w/v gelatin (Sigma-Aldrich, UK) into ice cube moulds, setting the moulds (4^{o}C) for 4 hours, and transferring to -80^{o}C for storage. The block was transferred from -80^{o}C to a -30^{o}C cryostat and the top cut down to produce an even surface. Using a pillar drill, nine 2.5x10mm holes were then drilled into the frozen block which was mounted in a cryostat set to -30^{o}C. SAOS-2 cells were trypsinised, counted, centrifuged and the supernatant removed. A range of doxorubicin concentrations (0, 0.031, 0.063, 0.125, 0.25, 0.5, 1, 2, 4 µM) were produced by mixing pelleted cells 2:1 with doxorubicin diluted in culture medium and placing the mixture in each cell plug hole, filling

an approximate volume of 49 µL, and stored in a sealed container in -80°C prior to MALDI-MSI.

Spheroid aggregates treated with 0, 0.16, 0.8, and 4 µM doxorubicin were harvested at 0 and 48 hours and embedded in 5% w/v gelatin + 2.5% carboxymethylcellulose (CMC) (Sigma-Aldrich, UK) inside a silicone mould, immediately frozen using liquid nitrogen and stored in air-tight containers. Sample sections were cut using the Leica 1850 UV cryostat (Leica Biosystems, UK), set to -30ºC, at 10 µm thickness, thaw mounted on a positively charged X-tra® adhesive slide (Leica Biosystems, UK) or on an Indium-Tin oxide (ITO)-coated slide (Visiontek Systems Ltd, UK), dependant on the analysis. All sample sections were taken straight after cryosectioning or from -80°C storage and immediately placed in a vacuum desiccator for ~15 minutes prior to matrix application. Negative mode imaging was performed with NEDC (Sigma-Aldrich, UK) (7 mg/mL, 50% MeOH) prepared as a matrix solution. The matrix was applied to the sample section using the SunCollect™ (Sunchrom, Germany) automated sprayer. Fifteen layers of matrix were applied, at 4 µL/min for the first layer and 3.5 µL/min for the remaining layers (speed x: low 7, speed y: medium 1, Z position: 35).

Imaging of the Doxorubicin spiked plug array and doxorubicin-treated spheroid aggregates was initially performed in negative mode using an Autoflex III, as it was equipped with a smartbeam laser which proved better for doxorubicin detection and was able to detect small molecules at lower spatial resolution settings. Negative ion mass spectra were acquired at a pixel size of 30 µm from *m/z* 50 – *m/z* 1000 in reflectron mode. The laser was focused to around 30 µm diameter. Four hundred laser shots were acquired for each spectrum. Data acquisition was performed using FlexControl (Bruker Daltonics, Germany), and visualizations were obtained from FlexImaging 4.0 (Bruker Daltonics, Germany).

MALDI-MSI of Doxorubicin-induced changes to endogenous metabolites in 3D cell culture

Treated spheroid aggregates (0, 0.8, 4µM) were sectioned as before at 10µm thickness, ensuring a section from the middle part of the spheroid aggregate was sampled. Three independent culture experiments were performed, and from each culture, three aggregated

spheroids were used, and three sections taken from each aggregated spheroid resulted in a total of 81 sections for MSI. The NEDC matrix deposition protocol used was as above.

Imaging of metabolite changes in response to Doxorubicin in spheroid aggregates was executed using a Synapt G2 (Waters, UK) in sensitivity mode as this instrument was capable of sufficient mass resolution and high enough throughput for the large sample comparison. Images of 60µm pixel size were acquired. Data was acquired over an *m/z* range of 50–1,000 in negative mode analysis. For positive mode imaging of doxorubicin inside a spheroid aggregate, images of 60µm were acquired at m/z 100-1200. The ion mobility function was used to improve separation of peaks. Data acquisition and analysis was performed using MassLynx v4.1 (Waters, UK) and High Definition Imaging (HDI) Software (Waters, UK). Tandem MS fragmentation was performed using an isolation window of 0.3 Da.

Regions of interest (ROIs) containing whole spheroid aggregates were selected in Waters HDI 1.4 imaging software and exported as average spectra into MassLynx software. They were then centroided and exported as .txt files and imported into Marker View software 1.2 (Applied Biosystems/MDS Sciex, Canada). An exclusion list to remove NEDC peaks was applied to the datasets, to remove the influences of the matrix signals when observing relationships of the treatment groups between spectra. The data were restricted to 5000 peaks and 0.1 minimum intensity and autoscaled. Principal Component Analysis-Discriminant Analysis (PCA-DA) was used to demonstrate that the spectral data could be used to visually discriminate between doses, and performed by informing the MarkerView software which samples belonged to each treatment group. The software then selected the two components that explained the most variance in normalised signal intensity over the peaks between groups.

Initially, a pragmatic approach was taken to analysing the data, aimed at balancing statistical rigour against time requirements for such high dimensional data with the software being used. Reduced Synapt data generated by the PCA-DA was initially put through a screening by *t test* comparison of each treatment group against each other. Potential effects of batch, culture and slice were ignored. The 50 peaks with lowest *P*-values for any comparison were then analysed further. The normalised signal intensities significantly deviated from the normal

distribution by Shapiro-Wilk tests. Therefore, Kruskal-Wallis tests were applied to each ionic species to determine if there was a significant effect of dose. This analysis was combined with Dwass-Steel-Chritchlow-Fligner *post-hoc* test when a significant difference was seen between treatment groups. Statistical analysis was performed using StatsDirect software (StatsDirectLtd, UK).

The inclusion of different batches, cultures and slices enables the variation due to these factors to be estimated and accounted for in statistical modelling, which increases the power to detect any dose effects. The data were exported from MarkerView R (v 3.4.1).[17] R is programmable software that enables a statistical test to be automated for very large numbers of variables. A linear mixed effect model was fit by restricted maximum likelihood for the normalised signal intensity of each peak using the function lme in package nlme (v 3.1-131)[18]. Batch and culture nested within batch were fitted as random effects and dose as a fixed effect [18]. An effect of dose was tested with an F test by applying the anova function to the fitted model object. The significance threshold was set to $P=1x10^{-5}$, which is a Bonferroni correction of $P=0.05$. Where a significant effect of dose was found, the model was re-run with the ordering of the levels of dose changed, to obtain P values from t tests of each pairwise comparison. The residuals from the model were also plotted against the fitted values to check they met the assumptions of a parametric analysis.

The significantly differing peaks discovered using either statistical approach were given putative assignments based on a database search in the Human Metabolome, Metlin or LipidMaps search databases. The error allowance used was 30ppm for small molecules and 0.01 Da for lipid identifications which was acceptable for the data acquired. Following the database search biological relevance was investigated within the possible identities within current literature.

Confirmation of Doxorubicin-induced metabolite changes by Fourier-Transform Ion Cyclotron Resonance (FT-ICR) MSI

To confirm the findings from the PCA study MALDI-FTICR-MSI of 0, 0.8 and 4µM doxorubicin-treated spheroid aggregates was performed on a 9.4T SolariX XR mass spectrometer (Bruker Daltonics, Germany) in negative-ion mode, using 200 laser shots per spot and 75 µm pixel size. Data was acquired in a *m/z* range from 50 to 1000 Da. For positive

mode imaging of doxorubicin inside a spheroid aggregate, 220 laser shots were used per spot at a 75µm pixel size. Data was acquired at m/z 100-1200. Data acquisition was performed using ftmsControl (Bruker Daltonics, Germany), and visualizations were obtained from flexImaging4.0 (Bruker Daltonics, Germany). As this instrument has a higher mass resolving power, both doxorubicin and the endogenous small molecules were clearer, however the method was only used to confirm due to large data sizes and analysis time requirements. The previously determined putative identifications were confirmed with the FTICR analysis within 3 ppm.

3 Results and discussion

Development of the SAOS-2 aggregated spheroid model

The SAOS-2 spheroid aggregate model was developed to allow sufficient spatial resolution of metabolites by MSI. Initial growth of SAOS-2 in alginate resulted in colonies typically 200 μM diameter, which may not provide sufficient information in low spatial resolution imaging experiments. To circumvent this problem, whilst keeping the presence of clonal heterogeneity, the alginate matrix was dissolved to release clonal tumour spheroids, which were subsequently aggregated in low-adhesion agarose-coated wells (Fig 1a). This process resulted in constructs of up to 1 mm. Staining of aggregated spheroids with Hoechst 33342, to localise all cells (blue), and propidium iodide, to localise regions containing necrotic cells (red) revealed heterogeneity across the tissue construct, with a clear viable rim containing no necrotic cells (Fig 1b). Caspase-3 is one of the executioner caspases at the end of the apoptotic cascade, and active caspase-3 is characteristic of apoptotic cell death and is present in regions of hypoxia in 3D cell cultures.[19] Staining for Caspase-3 activity using the NucView 488 fluorogenic Caspase-3 substrate revealed heterogeneous regions of apoptosis localised to the centre of the construct, whilst the viable rim remained devoid of active caspase-3. These results highlight the heterogeneous nature of aggregated spheroids, which contrasts with more uniform constructs generated from hanging-drop or aggregation of cell suspensions in low-adhesion plates.

Spatial distribution of endogenous metabolites within aggregated spheroids

MALDI-MSI of tumour spheroids revealed regional variations within the aggregated spheroids (Fig 2). Phosphoric acid (*m/z* 78.9493) was used to localise the aggregated spheroid construct. Detection of peaks with considerable variation in spatial distribution within the spheroid is evident, with *m/z* 426.0657 showing focal regions of detection, and *m/z* 281.2809 absent in the centre, and also at the periphery whereas localisation of *m/z* 403.1034 can be seen to localise within the central necrotic core region. Both *m/z* 158.9409 and *m/z* 606.0975 are largely absent from the viable rim region, with the latter showing evidence of delocalisation beyond the cellular construct, along with phosphoric acid.

SAOS-2 cells respond to doxorubicin, but not in 3D cell culture

Treatment of SAOS-2 cells with doxorubicin displayed a dose-dependent and time-dependent decrease in cell activity in 2D cell culture. Cell activity was reduced at 36 hours treatment compared to 12 hrs ($p < 0.0001$) with an IC_{50} of 1.09 µM after 36 hours (Fig 3a). In contrast, treatment of 3D aggregated spheroids resulted in no significant reduction of cell viability at doses up to 4 µM after 48 hours (Fig 3b). Impaired response to Doxorubicin in 3D cell culture is not unexpected, and hypoxia-induced resistance to doxorubicin has been reported in similar models.[20-21] It is well known that the central regions of MCTS are acutely hypoxic, resulting in apoptosis and necrosis,[22] which is consistent with observations seen in this model, and therefore likely accounting for observed lack of cytotoxic effects in this study.

To confirm Doxorubicin penetration into the 3D aggregated spheroid constructs, Doxorubicin distribution was determined by fluorescence microscopy. Since Doxorubicin fluoresces, drug distribution can easily be seen throughout the aggregated spheroid (red), as compared to Hoechst 33342 counterstain, which enters all cells (blue) (Fig 3c). After just 6 hours, 1 µM doxorubicin can clearly be seen staining cells within the spheroid aggregate, whereas post-staining with Hoechst 33342 shows only staining of the outer layer of cells, consistent with previous observations of Doxorubicin uptake in MCTS models.[23]

Cell plug arrays were made to aid detection of doxorubicin inside the spheroid aggregates. This was made by mixing SAOS-2 cells with doxorubicin standard and spiking these cells into a gelatin block. These could then be sectioned alongside the sample of interest and used as an internal standard array to demonstrate qualitative changes to doxorubicin within the sample (Fig 3).

Initial detection of Doxorubicin within the cell plug arrays was unsuccessful in positive mode by Q-TOF MS due to a close, interfering lipid peak (Fig 3d). The close interference within the spheroid aggregates was not significant at higher doxorubicin concentrations but once at a biologically relevant level, it was substantial. To achieve detection, alternative instrument types (FT-ICR) and negative mode were used enable visualisations. Putative doxorubicin could be observed in negative mode showing a promising increase in signal concurrent with an increase in doxorubicin signal intensity (Fig 3e).

Detection of endogenous metabolite changes in response to doxorubicin by MSI

In order to define the metabolomic and lipidomic spheroid aggregate response to Doxorubicin, 48-hour Doxorubicin-treated, and untreated spheroid aggregate sections were imaged in negative mode. The whole spheroid region was selected, and average spectra were extracted for comparison between groups. Comparison was performed using PCA-DA, which takes into account the group the sample belongs to and finds the principle components which separate these groups. The control and treatment groups were separated, and several species were separated out in the loading plot, in particular the 4µM treatment group (Fig 4).

Linear mixed effects analysis

The approach of using a combination of *t* tests within the MarkerView software to identify 50 peaks for follow-up testing by a Kruskal-Wallis test, found a significant effect of dose on the normalised signal intensity of 42 species. Some species were discarded as they were determined to be likely isotopes of other species. Linear mixed effects modelling, which accounts for variation due to batch and culture effects, found 24 species where the normalised signal intensity was significantly altered by dose. Of these, 18 were considered to be unique species (Table 1). Fitting linear mixed models also allowed the random variation in normalised signal intensity due to effects of batch and culture nested within batch, to be estimated. In several cases, one of these variances was negligible, and they were always smaller than the variation amongst slices. Theoretical accurate masses, measured masses and mass errors in ppm for the putative assignments are shown in Table 2. The assigned species were also confirmed within the FTICR imaging data. Ten ionic species (highlighted in Table 1) were detected as significant by both methods, which may be indicative of the strong significance of these ionic species in drug response. Results for 6 of these species based on intensities of the whole spheroid area are shown in fig 5. S-nitrosoglutathione (*m/z 335.0617*) (15 ppm) is known to modulate doxorubicin responses in breast cancer cells, whereby N-nitrosoglutathione suppressed doxorubicin activity.[24] N-nitrosylation, for which N-nitrosoglutathione is a mediator, is a key step in regulating DNA repair,[25] and observed changes likely reflect a DNA damage response. This molecule has been also been shown to induce increased expression of stress response genes and proteins.[26]

Putative identification of *m/z* 378.0869 (28ppm) as S-Lactoylglutathione, which was significantly increased in response to Doxorubicin, is of potential interest to the study of

osteosarcoma drug resistance. S-Lactoylglutathione is a known product of the Glyoxalase I (GLO1) enzyme, and is converted to D-lactate regenerating glutathione (Gillespie, 1978)[27]. A highly significant increase in ionic species *m/z 396.0996* was also found. This was putatively identified as S-Adenosyl-4-methylthio-2-oxobutanoate (3ppm) a factor of the modified methionine salvage pathway from 5'-methylthioadenosine (MTA) which could be of interest in cancer as a regulator of apoptosis and proliferation.[28] The lipids *m/z 714.5375*, putatively identified as PE(O-35:2) (0.0068Da); *m/z 758.4969*, identified as PS(34:2) (0.0009Da); *m/z 765.5488*, identified as PA(41:4) (0.0048Da); *m/z* 791.5778, and identified as PG(37:0) (0.0030Da) are not directly associated with any known osteosarcoma pathways or doxorubicin responses. However, *m/z 765.5488* showed a striking decrease and may be worthy of investigating as a possible marker of drug response.

MALDI-MSI (FT-ICR-MS) performed in negative mode aimed to validate changes in endogenous metabolites post-Doxorubicin treatment. Metabolomic species were originally acquired using the Synapt G2 and modelled by PCA-DA. Selected ionic species either identified as most highly significantly altered by Doxorubicin treatment, or species with putative identifications with potential relevance to cytotoxic drug responses. MSI is shown in Fig 6, and *m/z* 355.0617 is shown for comparison as it localised to the entire spheroid aggregate across all treatments. Highly consistent with PCA-DA findings (Fig 5), *m/z* 335.0617, putatively identified as S-nitrosoglutathione showed clear increase, as did *m/z* 378.0869 and *m/z* 396.0996 putatively identified as S-Lactoylglutathione and S-Adenosyl-4-methylthio-2-oxobutanoate respectively. Doxorubicin (*m/z* 542.1668) was identified within the same imaging experiment in negative mode, which increased in a dose-dependent manner with treatment, however was only readily detected in the centre of the spheroid where propidium iodide staining was typically observed. This may reflect an ability for Doxorubicin to ionise in intact *vs*. fragmented chromatin of necrotic and apoptotic cells. Ion species *m/z* 714.5375, 765.5488 and 791.5778 were all shown to be decreased by PCA-DA analysis, and subsequent FT-ICR MSI showed presence of all three putative lipids but with signals localised to the centre of the spheroid aggregates. Overall, these data show consistency with PCA-DA analysis of data obtained using Q-TOF and subsequent FT-ICR MSI imaging.

Concluding comments

In this study, we have developed a novel 3D cell culture model for osteosarcoma with cell constructs of sufficient size for spatial distribution of endogenous metabolites, and the ability to visualise heterogeneous metabolite distribution within the 3D constructs. We have demonstrated that within these constructs, we can visualise Doxorubicin, and despite the apparent lack of cytotoxic activity of Doxorubicin in 3D cell constructs *vs.* 2D cell culture, metabolomic changes can be imaged and identified using PCA-DA. As further validation of the species identified by PCA-DA analysis of Doxorubicin-treated spheroid aggregates, spatial distribution of changes of some of the most highly significantly altered metabolites followed similar patterns when independently analysed by FT-ICR. Some of the most highly significantly up-regulated species were putatively identified as metabolites of the glutathione system, and agents that modulate the glutathione system are known to modulate Doxorubicin activity.[29] In conclusion, MSI of drug-treated 3D cell cultures may identify biologically relevant metabolite changes highlighting this workflow as a potentially useful tool in *in vitro* drug discovery studies.

References

[1] S. Wei, L. Liu, J. Zhang, J. Bowers, G.A. Gowda, H. Seeger, T. Fehm, H.J. Neubauer, U. Vogel, S.E. Clare, D. Raftery. Metabolomics approach for predicting response to neoadjuvant chemotherapy for breast cancer. *Mol Oncol.* ***2013*** 7, 297-307. doi: 10.1016/j.molonc.2012.10.003.

[2] H. Jia, X. Shen, Y. Guan, M. Xu, J. Tu, M. Mo, L. Xie, J. Yuan, Z. Zhang, S. Cai, J. Zhu, Z. Zhu. Predicting the pathological response to neoadjuvant chemoradiation using untargeted metabolomics in locally advanced rectal cancer. *Radiother Oncol.* ***2018*** 128, 548-556. doi: 10.1016/j.radonc.2018.06.022.

[3] C. Bingel, E. Koeneke, J. Ridinger, A. Bittmann, M. Sill, H. Peterziel, J.K. Wrobel, I. Rettig, T. Milde, U. Fernekorn, F. Weise, A. Schober, O. Witt, I. Oehme. Three-dimensional tumor cell growth stimulates autophagic flux and recapitulates chemotherapy resistance. *Cell Death Dis.* ***2017*** 8, e3013. doi: 10.1038/cddis.2017.398.

[4] T.W. Fan, S.S. El-Amouri, J.K.A. Macedo, Q.J. Wang, H. Song, T. Cassel, A.N. Lane. Stable Isotope-Resolved Metabolomics Shows Metabolic Resistance to Anti-Cancer Selenite in 3D Spheroids versus 2D Cell Cultures. *Metabolites.* ***2018*** 8, pii: E40. doi: 10.3390/metabo8030040.

[5] N. Vidavsky, J.A.M.R. Kunitake, M.E. Diaz-Rubio, A.E. Chiou, H.C. Loh, S. Zhang, A. Masic, C. Fischbach, L.A. Estroff. Mapping and Profiling Lipid Distribution in a 3D Model of Breast Cancer Progression. *ACS Cent Sci.* ***2019*** 5, 768-780. doi: 10.1021/acscentsci.8b00932.

[6] S.F. Lan, B. Starly. Alginate based 3D hydrogels as an in vitro co-culture model platform for the toxicity screening of new chemical entities. *Toxicol Appl Pharmacol.* ***2011*** 256, 62-72. doi: 10.1016/j.taap.2011.07.013.

[7] C. Liu, Y. Liu, X.X. Xu, H. Wu, H.G. Xie, L. Chen, T. Lu, L. Yang, X. Guo, G.W. Sun, W. Wang, X.J. Ma, X He. Potential effect of matrix stiffness on the enrichment of tumor

initiating cells under three-dimensional culture conditions. *Exp Cell Res.* ***2015*** 330, 123-34. doi: 10.1016/j.yexcr.2014.07.036.

[8] A. De Luca, L. Raimondi, F. Salamanna, V. Carina, V. Costa, D. Bellavia, R. Alessandro, M. Fini, G. Giavaresi. Relevance of 3d culture systems to study osteosarcoma environment. *J Exp Clin Cancer Res.* ***2018*** 37, 2. doi: 10.1186/s13046-017-0663-5.

[9] D.R. Ahlf Wheatcraft, X. Liu, A.B. Hummon. Sample preparation strategies for mass spectrometry imaging of 3D cell culture models. *J Vis Exp.* ***2014*** 5, 94. doi: 10.3791/52313.

[10] D.R. Ahlf, R.N. Masyuko, A.B. Hummon, P.W. Bohn. Correlated mass spectrometry imaging and confocal Raman microscopy for studies of three-dimensional cell culture sections. *Analyst.* ***2014*** 139, 4578-85. doi: 10.1039/c4an00826j.

[11] B. Bakker, G.B. Eijkel, R.M.A. Heeren, M. Karperien, J.N. Post, B. Cillero-Pastor. Oxygen-Dependent Lipid Profiles of Three-Dimensional Cultured Human Chondrocytes Revealed by MALDI-MSI. *Anal Chem.* ***2017*** 89, 9438-9444. doi: 10.1021/acs.analchem.7b02265.

[12] X. Liu, A.B. Hummon. Mass spectrometry imaging of therapeutics from animal models to three-dimensional cell cultures. *Anal Chem.* ***2015*** 87, 9508-19. doi: 10.1021/acs.analchem.5b00419.

[13] X. Liu, C. Flinders, S.M. Mumenthaler, A.B. Hummon. MALDI Mass Spectrometry Imaging for Evaluation of Therapeutics in Colorectal Tumor Organoids. *J Am Soc Mass Spectrom.* ***2018*** 29, 516-526. doi: 10.1007/s13361-017-1851-4.

[14] M. Gaebler, A. Silvestri, J. Haybaeck, P. Reichardt, C.D. Lowery, L.F. Stancato, G. Zybarth, C.R.A. Regenbrecht. Three-Dimensional Patient-Derived In Vitro Sarcoma Models: Promising Tools for Improving Clinical Tumor Management. *Front Oncol.* ***2017*** 11, 203. doi: 10.3389/fonc.2017.00203.

[15] N.A. Cross, E.A. Waterman, N. Jokonya, A. Fowles, C.H. Buckle, J. Phillips, I. Holen, F.C. Hamdy, C.L. Eaton. Phenotypic variations of TRAIL sensitivity in cloned populations of prostate cancer cells. *J Cell Biochem.* ***2008*** 104, 1452-64. doi: 10.1002/jcb.21721.

[16] C.M. Hattinger, M. Pasello, S. Ferrari, P. Picci, M. Serra. (2010). Emerging Drugs for High-Grade Osteosarcoma. *Expert Opin. Emerg. Drugs.* ***2010*** 15, 615–634.

[17] R Development Core Team (2008). R: A language and environment for statistical computing. R Foundation for Statistical Computing, Vienna, Austria. ISBN 3-900051-07-0, URL http://www.R-project.org.

[18] J. Pinheiro, D. Bates, S. DebRoy, D., Sarkar, R Core Team (2019). nlme: Linear and Nonlinear Mixed Effects Models. R package version 3.1-140, https://CRAN.R-project.org/package=nlm

[19] S. Kessel, S. Cribbes, S. Bonasu, W. Rice, J. Qiu, L.L. Chan. Real-time viability and apoptosis kinetic detection method of 3D multicellular tumor spheroids using the Celigo Image Cytometer. *Cytometry A.* ***2017*** 91, 883-892. doi: 10.1002/cyto.a.23143.

[20] X. Song, X. Liu, W. Chi, Y. Liu, L. Wei, X. Wang, J. Yu. Hypoxia-induced resistance to cisplatin and doxorubicin in non-small cell lung cancer is inhibited by silencing of HIF-1alpha gene. *Cancer Chemother Pharmacol.* ***2006*** 58, 776-84.

[21] Y. Imamura, T. Mukohara, Y. Shimono, Y. Funakoshi, N. Chayahara, M. Toyoda, N. Kiyota, S. Takao, S. Kono, T. Nakatsura, H. Minami. Comparison of 2D- and 3D-culture models as drug-testing platforms in breast cancer. *Oncol Rep.* ***2015*** 33, 1837-43. doi: 10.3892/or.2015.3767.

[22] C.R. Thoma, M. Zimmermann, I. Agarkova, J.M. Kelm, W. Krek. 3D cell culture systems modeling tumor growth determinants in cancer target discovery. *Adv Drug Deliv Rev.* ***2014*** 69-70, 29-41. doi: 10.1016/j.addr.2014.03.001.

[23] J.K. Lukowski, E.M. Weaver, A.B. Hummon. Analyzing Liposomal Drug Delivery Systems in Three-Dimensional Cell Culture Models Using MALDI Imaging Mass Spectrometry. *Anal Chem.* ***2017*** 89, 8453-8458. doi: 10.1021/acs.analchem.7b02006.

[24] A. de Luca, N. Moroni, A. Serafino, A. Primavera, A. Pastore, J.Z. Pedersen, R. Petruzzelli, M.G. Farrace, P. Pierimarchi, G. Moroni, G. Federici, P. Sinibaldi, Vallebona, M. Lo Bello. Treatment of doxorubicin-resistant MCF7/Dx cells with nitric oxide causes histone glutathionylation and reversal of drug resistance. *Biochem J.* ***2011*** 440, 175-83. doi: 10.1042/BJ20111333.

[25] C.H. Tang, W. Wei, L. Liu. Regulation of DNA repair by S-nitrosylation. *Biochim Biophys Acta.* ***2012*** 1820, 730-5. doi: 10.1016/j.bbagen.2011.04.014.

[26] K.A. Broniowska, A.R. Diers, N. Hogg. S-nitrosoglutathione. *Biochim Biophys Acta.* ***2013*** 1830, 3173-81. doi:10.1016/j.bbagen.2013.02.004.

[27] E. Gillespie, Concanavalin A increases glyoxalase enzyme activities in polymorphonuclear leukocytes and lymphocytes. *J Immunol.* ***1978*** 121, 923-5.

[28] E. Albers. Metabolic Characteristics and Importance of the Universal Methionine Salvage Pathway Recycling Methionine from 5′-Methylthioadenosine. *IUBMB Life.* ***2009*** 61, 1132–1142.

[29] A.A. Mahbub, C.L. Le Maitre, S.L. Haywood-Small, N.A. Cross, N. Jordan-Mahy. Glutathione is key to the synergistic enhancement of doxorubicin and etoposide by polyphenols in leukaemia cell lines. *Cell Death Dis. 2015* 31;6:e2028. doi: 10.1038/cddis.2015.379.

Ionic species (m/z)	*P value*	Putative identification
180.4920	4.57x10-6	
245.0544*	1.68x10-7	
253.2270	9.89x10-6	
331.0550*	3.48x10-11	
335.0617*	<1.00x10-12	S-nitrosoglutathione
347.0637*	1.14x10-7	
364.0735	1.49x10-9	2-S-glutathionyl acetate
378.0869*	2.62x10-11	S-lactoylglutathione
396.0996*	<1.00x10-12	S-Adenosyl-4-methylthio-2-oxobutanoate
404.0321	1.61x10-7	
414.1022*	<1.00x10-12	
464.0080	1.29x10-6	
565.9493	1.05x10-6	
583.9583	5.98x10-6	
589.9554*	1.92x10-7	
714.5375	9.77x10-8	PE (O-35:2)
765.5488*	1.25x10-10	PA (41:4)
791.5778*	3.10x10-7	PG (37:0)

*Table 1: Ionic species with a significant effect of dose on normalised signal intensity as tested by a mixed effects model. The significance threshold was set to P<1x10-5. * indicates species that were also identified by the combination of t test and Kruskal-Wallis test.*

Experimental mass (*m/z*)	Theoretical mass (*m/z*)	Mass error (ppm)	Assignment
335.0617	335.0667	15	S-nitrosoglutathione
364.0735	364.0820	23	2-S-glutathionyl acetate
378.0869	378.0977	28	S-lactoylglutathione
396.0996	396.0983	3	S-Adenosyl-4-methylthio-2-oxobutanoate
714.5375	714.5443	10	PE (O-35:2)
765.5488	765.5440	6	PA (41:4)
791.5778	791.5808	4	PG (37:0)
858.8311	858.8284	3	1-O-behenoyl-Cer(d34:1)

Table 2: Theoretical accurate masses, measured masses and mass errors in ppm for the putative assignments.

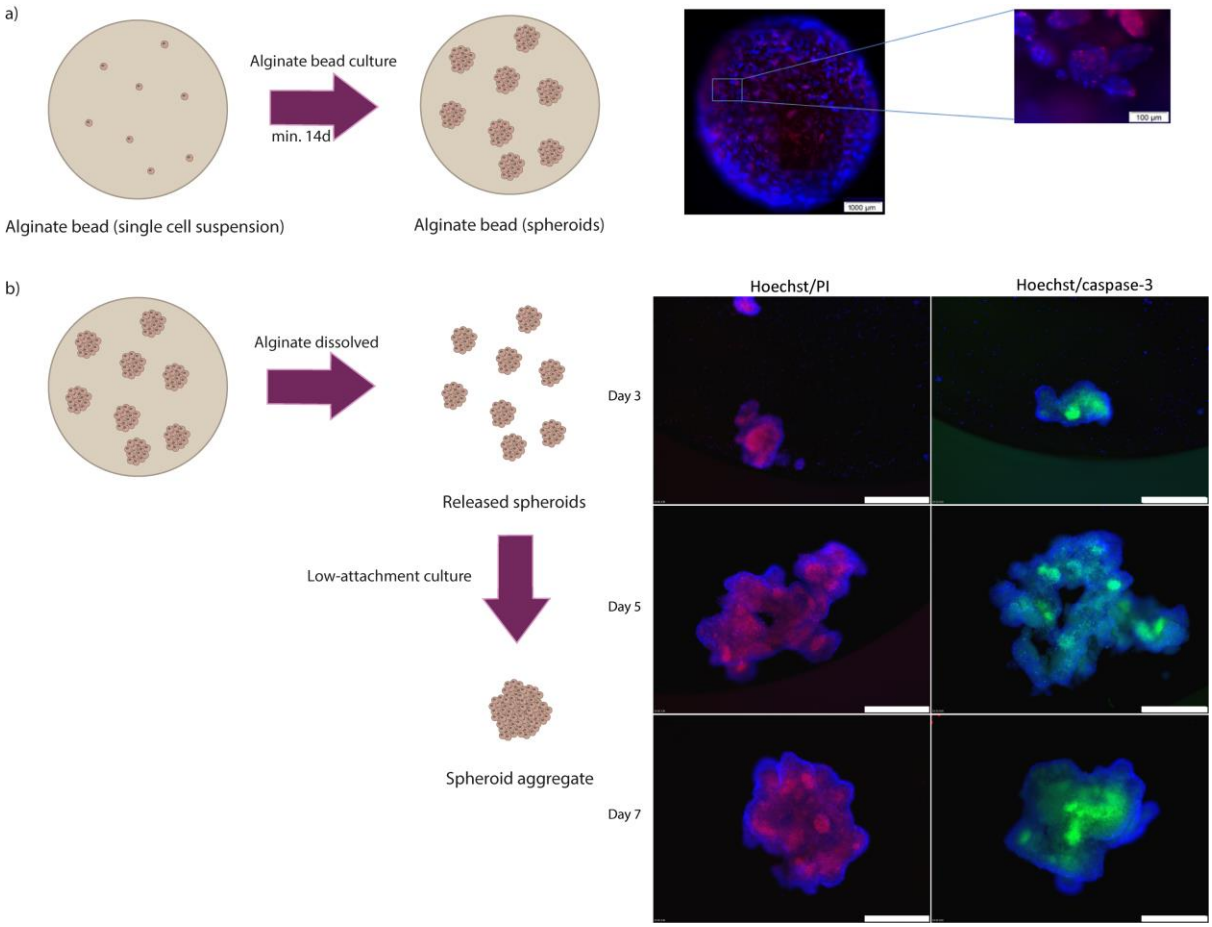

Figure 1: *Generation of aggregated spheroid model. a) Cells are suspended in alginate and clonal proliferative colonies form. Hoechst 33342 identified all cells and Propidium Iodide identifies regions containing dead cells. b) After alginate dissolution, spheroids are aggregated in a low-adhesion well. Hoechst 33342 and Propidium iodide staining highlights a viable rim with necrotic or dead cells present within the construct, co-localised with caspase-3 activity confirming presence of apoptotic cells within the core. Scale bar=500 µm.*

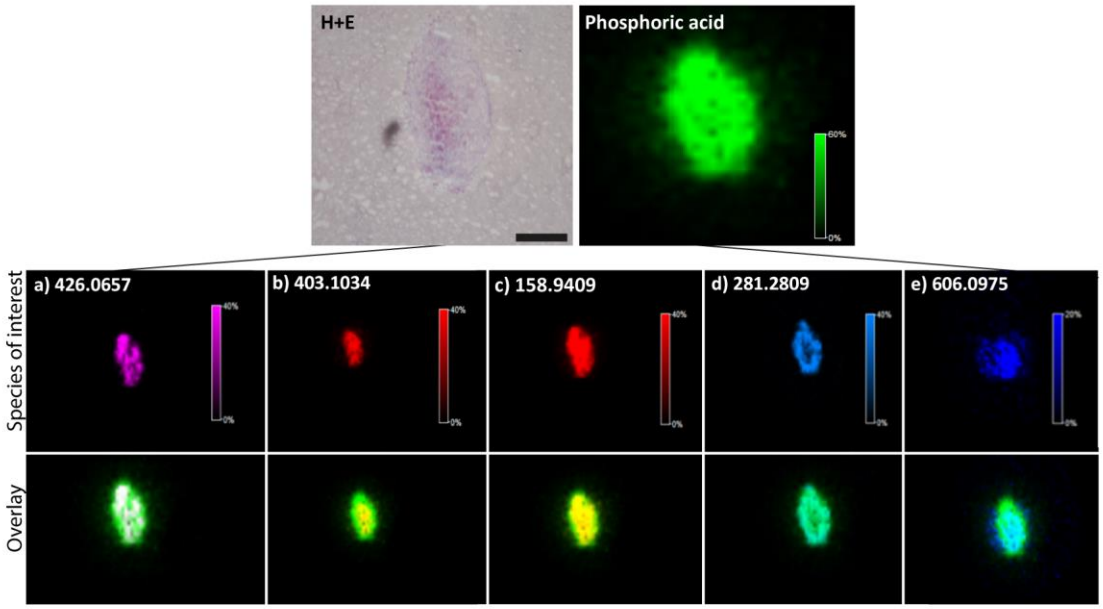

Figure 2: *Detection and localisation of endogenous metabolites aggregated spheroid model by MSI using Bruker Autoflex III. Haematoxylin and Eosin staining shows the outline of the aggregated spheroid (scale bar = 500 µM). Phosphoric acid (m/z 78.9493) is ubiquitously present and outlines the aggregated spheroid by MSI. Overlay of phosphoric acid and endogenous metabolites shows heterogeneity of detection within the aggregated spheroid.*

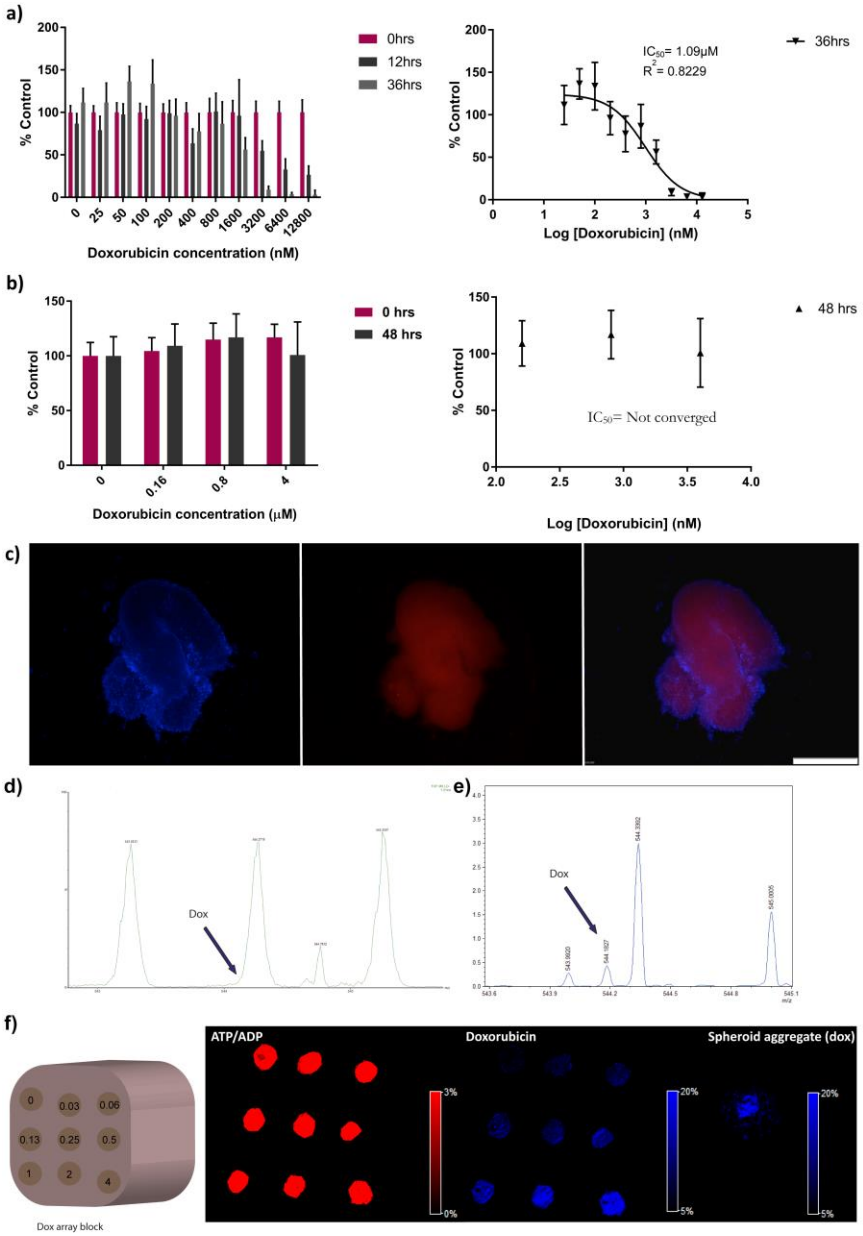

Figure 3: *Effects of Doxorubicin on SAOS-2 cells. a) SAOS-2 cells responded to doxorubicin treatment in 2D cell culture, as determined by Resazurin assay. b) SAOS-2 did not show significant reduction in activity after treatment with Doxorubicin at doses in excess of the IC_{50} value determined from the 2D culture. c) Fluorescence microscopy of Hoechst 33342 staining (blue), and Doxorubicin (red) localisation throughout aggregated spheroid, confirming drug uptake into the aggregated spheroid. Scale bar = 500 µM. d and e) Detection of Doxorubicin in positive mode m/z 544.1827 by FT-ICS-MS (e), whereas this was not visible by Q-TOF (d) due to a close interfering peak. f) Detection of doxorubicin in negative mode in the cell-spiked array plug vs. ATP/APD for cellular co-localisation. Presence of Doxorubicin in a 4µm-treated spheroid aggregate is shown.*

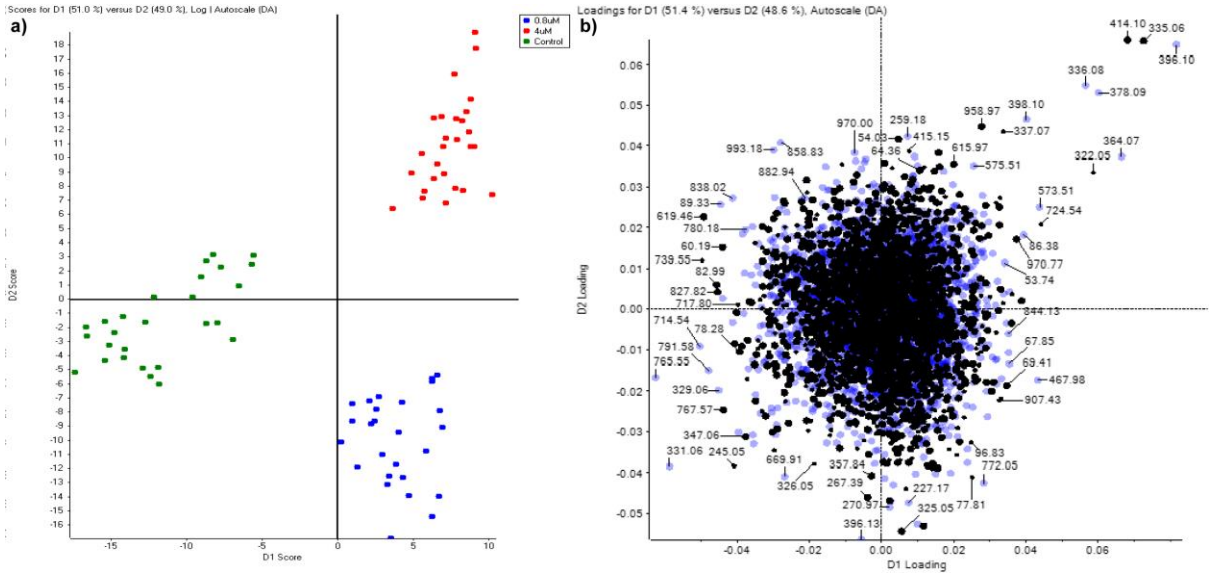

Figure 4: *a) PCA-DA loading plots showing clear separation by dose and b) the weighting chart of all ionic peaks, with peaks that make a large contribution to the principle components being found in the periphery of the main cluster.*

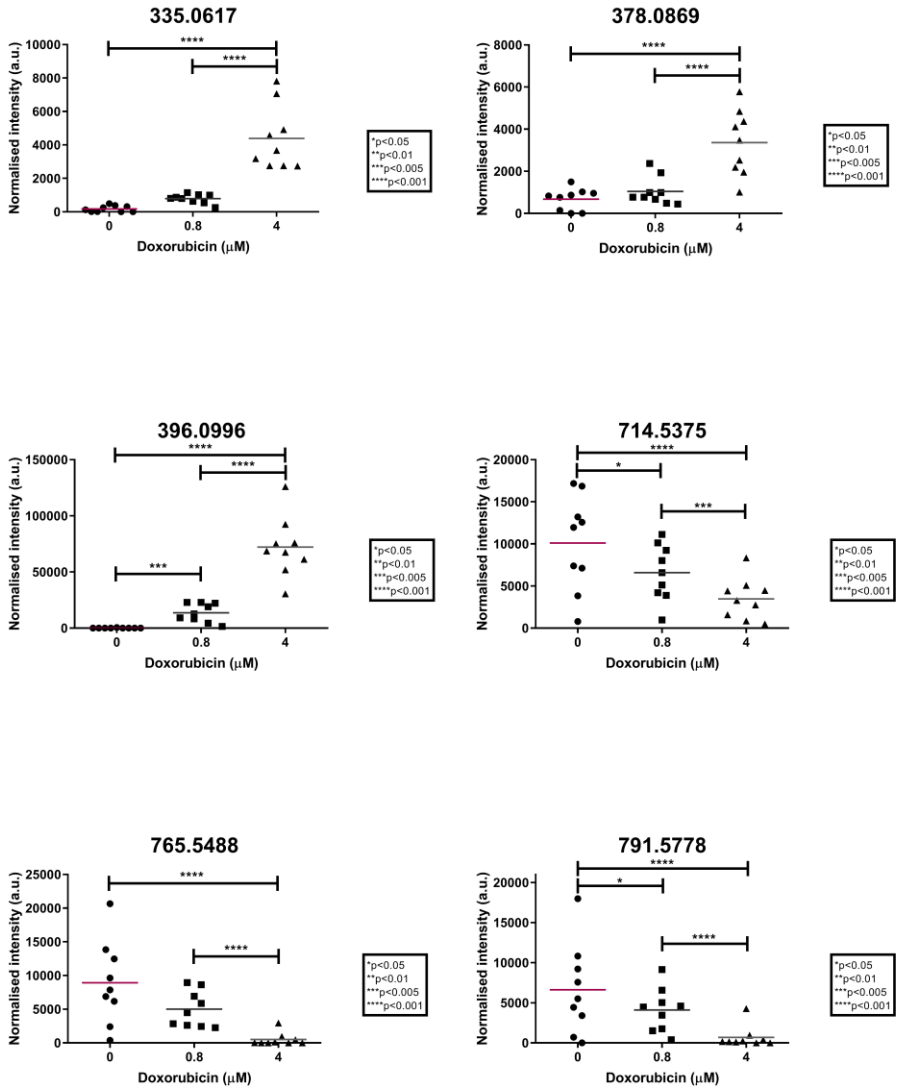

Figure 5: *Normalised signal intensity of six ionic peaks at 0, 0.8 and 4 μM Doxorubicin treatments. Data is from three independent batches, with three sections analysed for each experiment. Significant differences between pairs of doses from t tests within a linear mixed model are indicated. Fitted values for each dose from the linear mixed model are shown as horizontal lines across the data.*

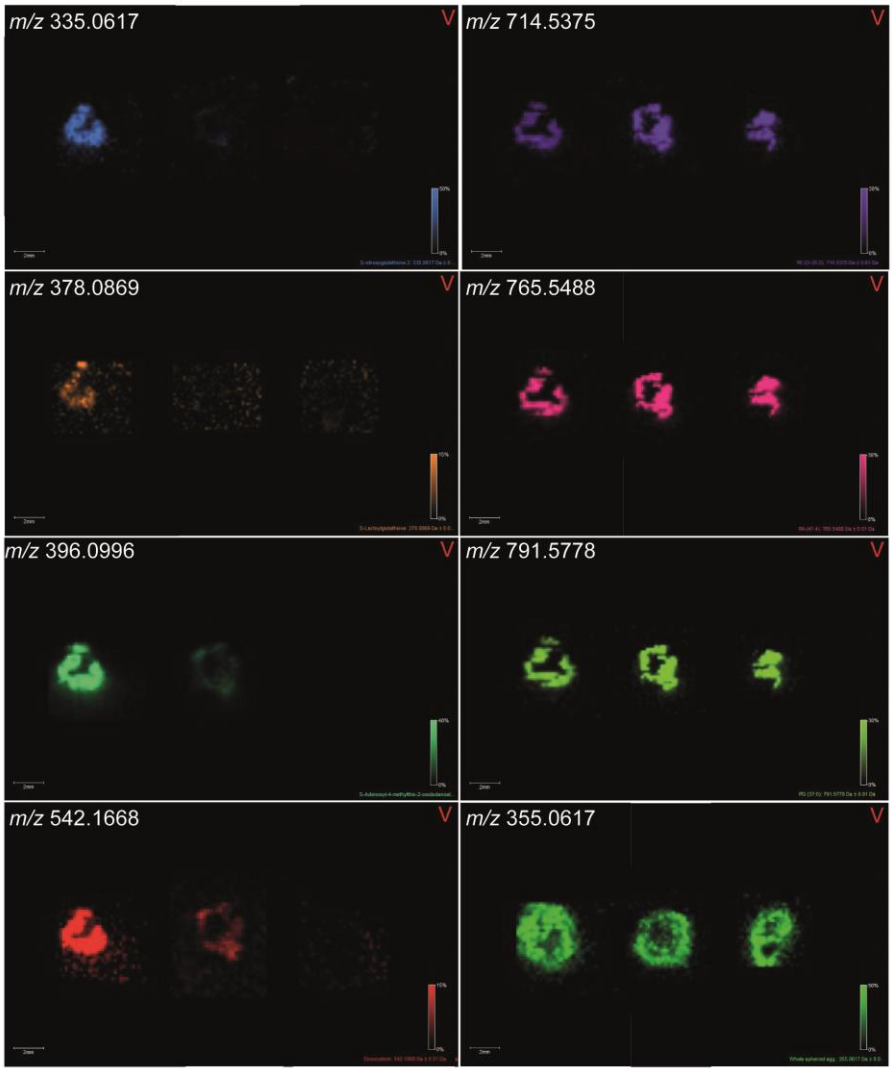

Figure 6: *Negative mode FT-ICR MSI of selected targets altered by Doxorubin and initially identified by PCA-DA. Treatment groups are 4 µM, 0.8 µM and control. m/z 355.0617 identified the whole spheroid aggregate, and m/z 542.1668 is Doxorubicin, which shows predominant localisation in the centre of the spheroid. m/z 335.0617, m/z 378.0869 and m/z 396.0996 show striking increased in response to Doxorubicin, consistent with PDA-DA analysis. The remaining species are putatively identified as lipids and show a similar spatial distribution.*